Applied Medical Informatics
Original Research Vol. 37, No. 4 /2015, pp: 38-50

The Complete Local Spatial Central Derivative Binary Pattern for Ultrasound Kidney Images Retrieval

Chelladurai CALLINS CHRISTIYANA[1,*] and Vayanaperumal RAJAMANI[2]

[1]Department of Computer Science and Engineering, Sethu Institute of Technology, Madurai, Tamilnadu, India
[2]Department of Electronics and Communication Engineering, Veltech Multitech Dr. Rangarajan Dr. Sakunthala Engineering College, Chennai, Tamilnadu, India
E-mails: callinschristiyana_c@yahoo.co.in; rajavmani@gmail.com

* Author to whom correspondence should be addressed; Tel.: +91-99650 90567

Received: October 18, 2015 / Accepted: December 1, 2015 / Published online: December 15, 2015

Abstract
The Content Based Image Retrieval (CBIR) is an active research domain in medical applications. The feature extraction process is the vital procedure in CBIR. This work proposes a new feature extraction procedure named as Complete Local Spatial Central Derivative Binary Pattern (CLSCDBP) for ultrasound kidney images retrieval. In a local 3X3 square region of an image, the new pattern considers the relationships among the surrounding neighbors about their neighbors at different spatial distances whereas the standard Local Binary Pattern reflects the relationships between the center pixel and the surrounding neighbors. Though the surrounding neighbor pixels relationship has been considered in the Local Mesh Peak Valley Edge Patterns (LMePVEP), the proposed feature is different by deriving the local pattern based on the encoding of central derivative of the surrounding neighbors of the center pixel. The neighbors of each surrounding pixel in different spatial distances are considered during central derivative computation. The proposed local pattern becomes complete by accompanying the global mean statistics into it. The performance of this new feature is examined in ultrasound kidney images retrieval system. The experimental results confirm that CLSCDBP achieves considerable step up in the retrieval of ultrasound kidney images than LMePVEP in terms of Retrieval Efficiency.

Keywords: Content Based Image Retrieval (CBIR); Texture; Local Patterns; Local Binary Pattern (LBP); Local Mesh Peak Valley Edge Patterns (LMePVEP); Ultrasound kidney images; Retrieval efficiency

Introduction

Every day, numerous amounts of medical images are generated in hospitals and medical centers. The medical images which are collected in various formats such as MRI, CT, PET, ultrasound and X-ray are stored in medical image databases for future reference. The applications of these images are enormous. The medical images can be used for patient diagnosis, citation and surgery process. These medical images should be properly indexed to make use of them into above said applications. The proper indexing method allows the user to access, search and retrieve the required images from medical image databases. The indexing can be facilitated by the technique called Content Based Image Retrieval (CBIR). CBIR groups the similar images from the database based on their visual content [1, 2]. CBIR in medical application is called as Content Based Medical Image Retrieval

(CBMIR).

CBIR method yields the results by means of the processes called as feature extraction, similarity matching and retrieval. Feature extraction process is the key process in CBIR since it extracts the visual contents from the image. The performance of the CBIR system is depended upon the feature extraction process which is used in the system. The extracted features are arranged in the feature vector by the feature extraction process. The feature vector is the visual content representation of the image. The visual content of the image is normally represented by means of low level features such as color, texture and shape. The features may be extracted in global or local manner. Once the feature vectors of the images are formed, they are compared by similarity matching procedure. Any one of the distance measures like Euclidean distance, Chi-square distance, Canberra distance and many more can be used for the similarity matching process. The image retrieval process collects the similar content images together based on the feature vectors distance.

There are umpteen numbers of works in medical applications which imbibes in it the CBIR technique [3]. Every work is differentiated in the manner of methodology of feature extraction procedure, distance measure which is used in the similarity matching scheme or the medical image databases which are taken for analysis. The feature extraction procedure may use the single visual feature or collection of visual features to represent the content of an image. Among the visual features of an image, the texture feature plays a significant role in medical image analysis [4], since; it represents the image content and delivers the semantic information.

There are many number of CBIR system in medical applications which was developed based on the various texture representation methods. Some studies are discussed as follows. Landeweerd et al. [5] distinguished different kinds of white blood cells using first order and second order statistics. Chen et al. [6] derived fractal texture features for the classification of ultrasound liver images. Stavroula et al. [7] used first order statistics, spatial gray level dependence matrix, gray level difference method, laws texture energy measures and fractal dimension measurements to classify liver tissue from non-enhanced CT images. Manikandan et al. [8] have drawn second order statistical texture features from GLCM for the retrieval of ultrasound kidney images. Baopu Li et al. [9] have applied curvelet transformation and extracted Local Binary Pattern to identify ulcer regions in capsule endoscopy images. Sang Cheol Park et al. [10] have extracted 14 morphological features, intensity distribution feature and fractal dimension measure for the classification of suspicious breast masses from the breast images. El-Sayed Ahmed El-Dahshan et al. [11] have employed Discrete Wavelet Transformation (DWT) to classify the Magnetic Resonance Images (MRI). Quellec et al. [12] have applied Optimized wavelet transform for Medical images retrieval. Sohail et al. [13] have developed retrieval and classification system for ultrasound medical images of ovarian system using histogram moments and GLCM based texture features. Júlia E.E. de Oliveira et al. [14] have used two dimensional Principal Component Analysis technique to retrieve mammographies from large medical image database.

Kehong Yuan et al. [15] have exploited Non-negative tensor factorization technique to build the brain CT image database. Zare et al. [16] have used GLCM, Canny Edge Operator, Local Binary Pattern and pixel level information to classify the medical X-ray images. Yu-Ying Liu et al. [17] have analyzed optical coherence tomography (OCT) images with global and local descriptors. Rodrigo Pereira Ramos et al. [18] designed the CAD system for digitized mammograms through GLCM, wavelet and ridgelet transforms. Muthu Rama Krishnan et al. [19] have detected benign/malignant oral lesions from histopathological images using Higher Order Spectra (HOS), Local Binary Pattern (LBP), and Laws Texture Energy (LTE) features. Callins Christiyana et al. [20] have derived statistical texture features from grey level difference histogram for ultrasound kidney images retrieval. Kumar et al. [21] have identified both benign and malignant liver tumors on CT images via GLCM, wavelet and contourlet coefficient statistics. Shichong Zhou et al. [22] have extracted Shearlet-based texture features for the classification of breast tumor in ultrasound images. Callins Christiyana et al. [23] have derived second order statistical texture features from CSLBPGLCM for the retrieval of ultrasound kidney images. Bi Bi et al. [24] have presented H-LBP feature for Edge extraction in blurry Digital Radiography (DR) images.

The best texture representation method among the various methods is selected based on its efficiency. The efficient method should be computationally simple and have good discrimination power. The Local Binary Pattern (LBP) [25] is the method which satisfies the above said qualities. In a small square region, the LBP feature finds the binary pattern based on the grey level intensity relation between the center pixel and its surrounding neighbors. Though the simple LBP is superior which itself has some crisis [26]. To address this concern, many LBP variants were proposed. The LBP variants such as Local Ternary Patterns (LTP) [27], Local Quinary Pattern (LQP) [28] and Local Derivative Pattern (LDP) [29] were used in many applications.

The extensions and variants of LBP are applied in the numerous medical domain applications. Some of them are imparted as follows. Shao-Hu-Peng et al. [30] have presented ELBPriu4 and gradient orientation difference feature for the detection of pathological change in the chest CT images. Subrahmanyam Murala et al. [31] have devised Directional Binary Wavelet Pattern (DBWP) for the retrieval of MRI and CT images. In DBWP, the grey scale image is divided into 8 binary bit planes in which the Binary Wavelet Transform (BWT) is applied. The LBP features are extracted from the resultant Binary Wavelet Transform (BWT) sub-bands. Ashish oberoi et al. [32] have used Local Tetra Patten (LTrP) for the retrieval of retinal images. The LTrP finds the relationship between the center pixel and the surrounding neighbors using first order and second derivatives calculated in vertical and horizontal directions. Subrahmanyam Murala et al. [33] have formulated Local Ternary Co-occurrence Pattern (LTCoP) for the retrieval of MRI and CT images. The LTCoP encodes the co-occurrence of local ternary edges in the adjacent neighborhood of the small square region considered. Ryusuke Nosaka et al. [34] have offered novel method for classifying six categories of patterns of fluorescence staining of a HEp-2 cell. This method is constructed as a combination of the rotation invariant co-occurrences among the adjacent local binary pattern (RIC-LBP) image feature and a linear support vector machine (SVM). Recently, Subrahmanyam Murala et al. [35] have presented Local Mesh Peak Valley Edge Patterns (LMePVEP) for MRI and CT images indexing and retrieval purpose. This work is entirely different from the previously described works in the manner of computing the local patterns. The LMePVEP extracts the relationships among the neighbors of the center pixel in a given square region rather than computing the relationships between the center pixel and the surrounding neighbors. The LMePVEP encodes the co-occurrence of forward and backward derivatives among the surrounding neighbors in the different spatial distance for a given center pixel. The performance of the LMePVEP is proved superior when it is compared with earlier local patterns. The literature study gives that the LMePVEP is different from all the other LBP variants since it is the only pattern which considers the relationship among the surrounding pixels of the center pixel in a local region.

The LMePVEP also has its own drawbacks. There are two issues. The first issue is the computational efficiency of the LMePVEP. The LMePVEP pattern increases the computational barrier in spite of involving every surrounding pixel of a local region twice in the forward and backward derivative computation at a particular spatial distance. The second issue is the absence of global statistics in the local pattern. None of the local pattern in the literature study incorporates the global information in it. Due to this reason, the two different textures are sometimes recognized as similar [36]. The new feature is proposed in the aim of addressing the two issues. This work proposes the feature which also considers the relationships among the pixels of a local region in compliance with the LMePVEP. In the proposed work, the polarity of central derivative of every surrounding neighbors of the center pixel at different spatial distance is encoded into binary pattern to reduce the computational barrier of LMePVEP. The cost of the computation is reduced into half by this way. In addition to that, the computed local pattern is classified into two in order to accompany the global information. The resulting new local texture pattern is named as Complete Local Spatial Central Derivative Binary Pattern (CLSCDBP). This is the complete pattern because in every local region the global information is also accommodated. The aim of this manuscript was to apply the CLSCDBP pattern as the feature extraction technique in ultrasound kidney image retrieval system and to prove its proficiency over LMePVEP Pattern.

The Proposed Complete Local Spatial Central Derivative Binary Pattern (CLSCDBP) Formation

This section illustrates the computation of the CLSCDBP feature in a 3×3 local region as well as the image retrieval process using the CLSCDBP feature vector.

Computation of the Proposed Pattern

The CLSCDBP pattern extracts the relationships among the surrounding pixels in the neighborhood of the given center pixel. The sample 3X3 square region with the labeling of the center pixel and its surrounding neighbors are given in the Figure 1.

A	B	C
H	CP	D
G	F	E

Figure 1. A Sample 3×3 square region

In Figure 1, the CP is the center pixel of the region. The pixels A, B, C, D, E, F, G and H are the surrounding neighbors of the pixel CP in the neighborhood. The relationships among these pixels are considered in the new pattern calculation. The proposed work employs the central derivative concept when it finds the relationship among the surrounding pixels of the given center pixel. For every pixel in the surrounding neighborhood, there are two possible neighbors in three different distances such as d=1, 2 and 3. The surrounding pixel A in the Figure 1, has two neighbors (H, B), (G, C) and (F, D) at distances 1, 2 and 3 respectively. The comparison of forward, backward and central derivatives are presented in [37]. From the study, it is perceived that the central derivative formulas are more accurate and produce the smallest methodological errors than forward and backward derivatives. So, it is significantly better to use the central derivative.

To include the global information into the calculated local pattern, the pattern is categorized into two, based on the relationship between the global mean intensity and the local region mean intensity. The mean statistics is more robust in all the other statistical parameters since it is least affected by the outliers [36].

Based on the above description, the computation of CLSCDBP is described as follows. For every surrounding pixel g_c in the neighborhood of 3×3 region, the central first order derivative with its predecessor and successor neighbors at distance 1, 2 and 3 is calculated using the Equation 1.

$$\mathrm{GFOD}(g_{p,1}) = g_{p,i} - g_{s,i} \mid \mathrm{I} = 1, 2, 3 \tag{1}$$

where $\mathrm{GFOD}(g_{p,1})$ is the central first order derivative of the pixel ; g_c with distance *i* neighbors. The terms $g_{p,i}$ and $g_{s,i}$ are the predecessor and successor neighbors at distance i^{th} respectively. The CLSCDBP with distance *i* for the given 3×3 square region is computed based on the Equation 2.

$$CLSCDBP(CP \mid i) = \sum_{j=1}^{8} T(CFOD(g_{j,i})) \times 2^{j-1} \mid i = 1,2,3 \tag{2}$$

where T is the binary threshold function which is interpreted using the Equation 3.

$$T(x) = \begin{cases} lifx \geq 0 \\ 0 \quad otherwise \end{cases} \tag{3}$$

The computed patterns in all the three distances in the local region are classified into two groups based on the comparison between global mean intensity with the local region mean intensity. The computational illustration of CLSCDBP for the 3×3 region with 3 distance neighbors is given in the Figure 2.

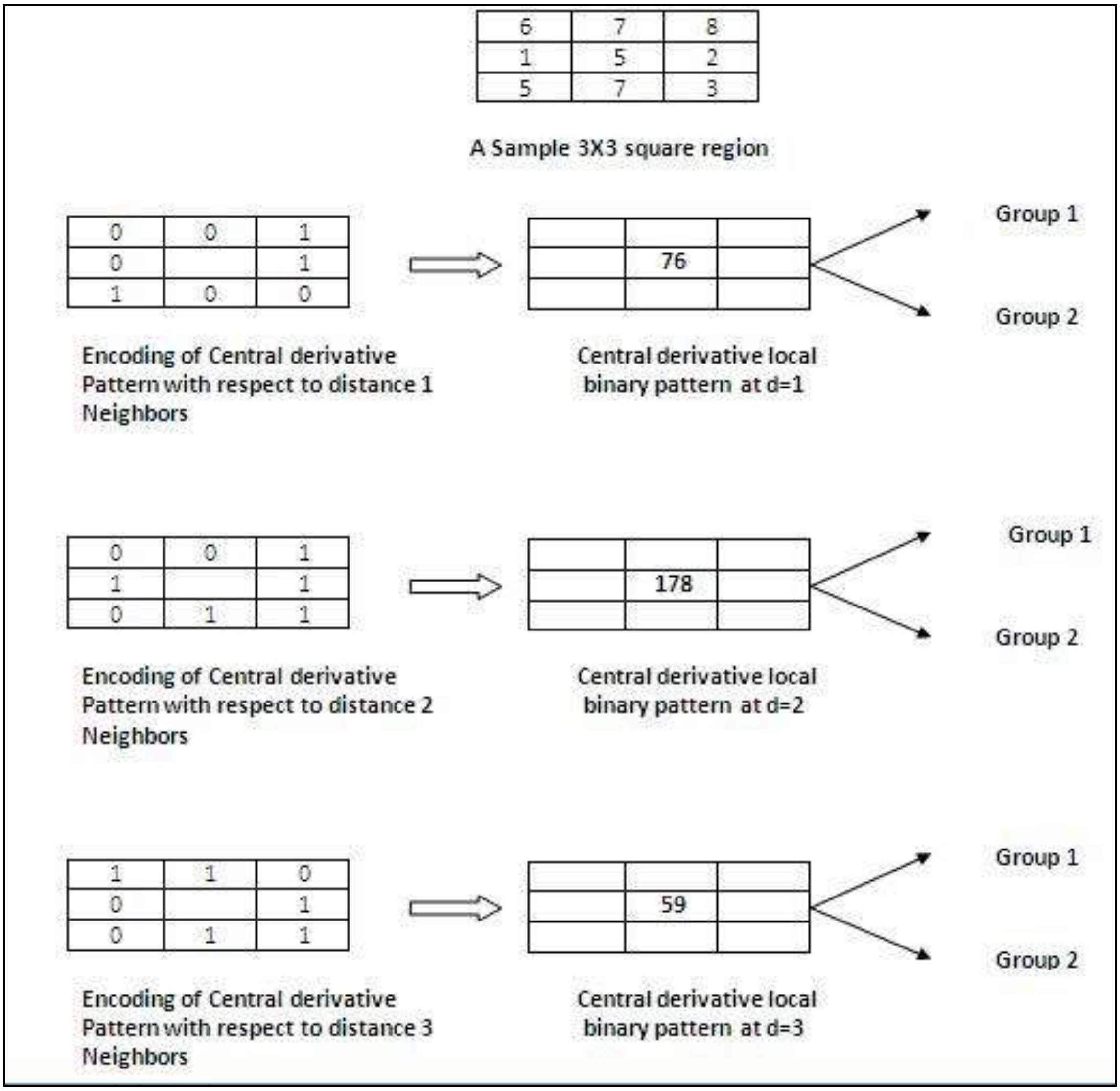

Figure 2. Computation of Complete Local Spatial Central Derivative Local Binary Pattern

Image Retrieval Algorithm using CLSCDBP Feature

The image retrieval algorithm with the proposed CLSCDBP is given in the subsequent steps. The algorithm inputs the query image and supplies similar content images from the database as the output. The algorithm assumes that the feature vector formation of database images is done in offline and considers there are N images in the database. The steps are as follows:

1. Input a query image.
2. With respect to every pixel of a query image as a center pixel, two classes of CLSCDBP in three distances such as d=1,2 and 3 are formed.
3. Construct the histograms of all the six possible classes of CLSCDBP for a query image. The six histograms are linearly concatenated to form a feature vector (of length 1536) of a query image.
4. Set the threshold value.
5. For i=1 to N do
    i. Compare the feature vectors of the query image and ith image in the database using the prescribed distance measure.
    ii. If the comparison result is within the threshold limit, then the ith image in the database is retrieved as similar to the query image.

The Feature vector formation of concatenated CLSCDBP histograms for an ultrasound kidney image is given in the Figure 3.

a) b)

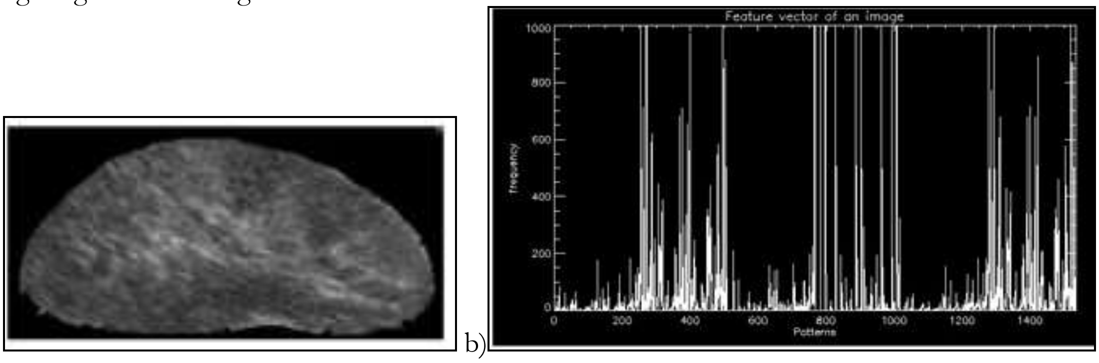

Figure 3. Feature Vector Formation of an image using CLSCDBP: a) ultrasound kidney image; b) feature vector formation of the image a) using CLSCDBP patterns

Similarity Matching

Similarity matching process is the crucial part in the image retrieval system since it decides the output of the system. The two factors affect the results of an image retrieval system normally. They are: feature extraction algorithm and similarity measure. This work employs the CLSCDBP feature for image content representation. The feature vector of an image F= (f1 to fn | n=1536) is framed by concatenating six possible histograms of each length 256. The similarity measure which is applied to an image retrieval system depends on either the nature of the feature vector or the test bed images. The chi square distance metric [38] is more suitable for similarity matching process of histogram oriented feature vectors. The chi-square distance measure is given in Equation 4.

$$D(x,y) = \sum_{i=1}^{n} \frac{(x_i - y_i)^2}{x_i^2 + y_i^2} \qquad (4)$$

where D(x,y) in the Equation 4 is the chi-square distance between the feature vectors of the query image(x) and the database image(y).

Experimental Results and Discussions

This work designs the CLSCDBP based image retrieval system for ultrasound kidney images. The performance of the CLSCDBP is compared with the LMePVEP, since, the LMePVEP feature is proved as the best among the local patterns. The database of different categories of ultrasound kidney images like Normal, Cortical Cysts (CC) and Medical Renal Diseases (MRD) are considered in the performance evaluation of CLSCDBP based image retrieval system. The ultrasound kidney images which are used in this analysis are acquired by using scanning systems ATL HDI 5000 curvilinear probe with transducer frequency 5-240 MHz and Wipro GE LOGIQ 400 curvilinear probe with transducer frequency 3-5 MHz. Transducer frequency at 4 MHz is fixed for taking the longitudinal cross section of the kidney. The image retrieval is done by inputting a query image to the system and collects the similar images from the database. Every image in the database is acted as a query image.

The efficiency of the image retrieval system is evaluated by two familiar measures such as Precision and Recall [39]. The precision and recall values of the query image q is denoted as P(q) and R(q) respectively. They are computed using the Equations 5 and 6.

$$P(q) = \frac{Number\ of\ relevant\ images\ retrieved}{Total\ number\ of\ images\ retrieved} \quad (5)$$

$$R(q) = \frac{Number\ of\ relevant\ images\ retrieved}{Total\ number\ of\ images\ retrieved\ in\ database} \quad (6)$$

The precision and recall values of an individual query image at various thresholds are measured in the range of 0 to 1. The average value of them at every threshold is recorded. This work considers the number of top images retrieved as the threshold value. The performance analysis of the image retrieval systems with top 100 images retrieved in the interval of 10 is analyzed. Precision at smaller thresholds is very important in medical applications since every physician wants to access the top relevant results. Recall at smaller thresholds gives petty information for the queries with many relevant images in the database. The precision analysis of the three categories of ultrasound kidney images with top 100 images retrieved in the interval of 10 are shown from the Figure 4 to Figure 6. The recall values of top 100 images retrieved for the combined databases with two features are presented in the Figure 7. The top 5 images which are retrieved by these two systems with a sample query image are given in the Figure 8.

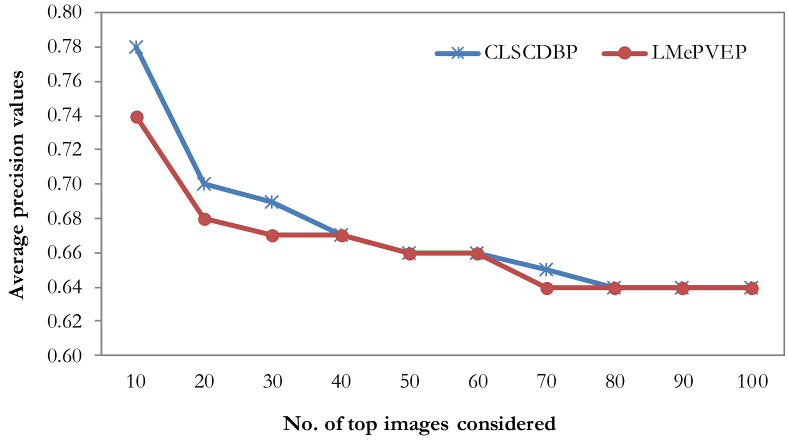

Figure 4. Precision value comparison of normal ultrasound kidney images

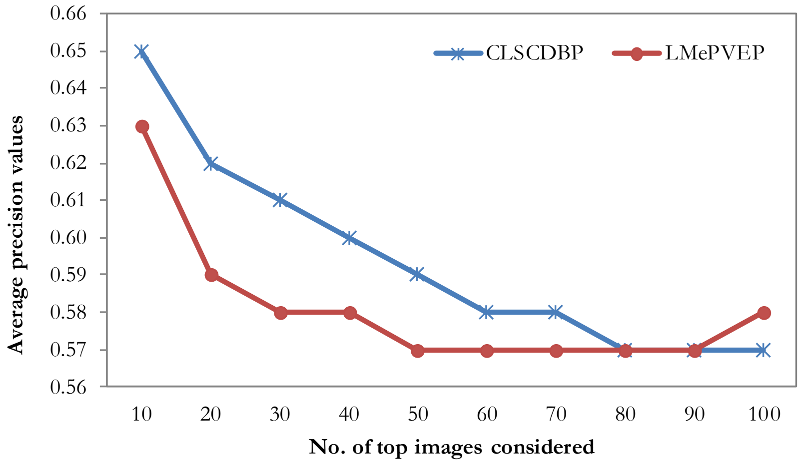

Figure 5. Precision value comparison of CC ultrasound kidney images

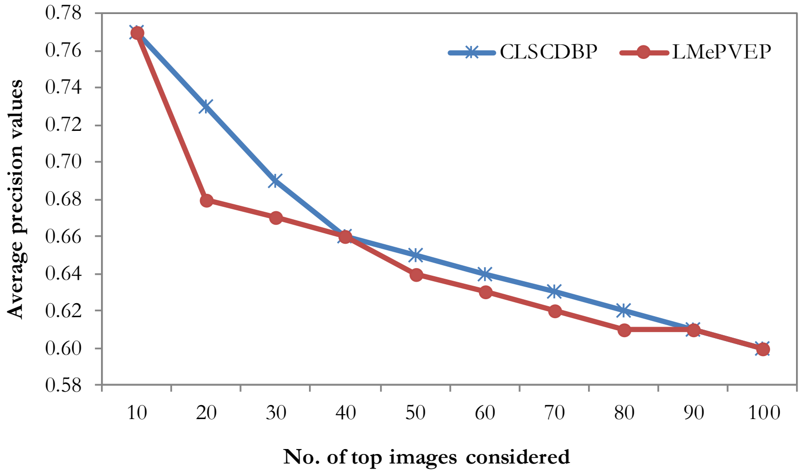

Figure 6. Precision value Comparison of MRD ultrasound kidney images

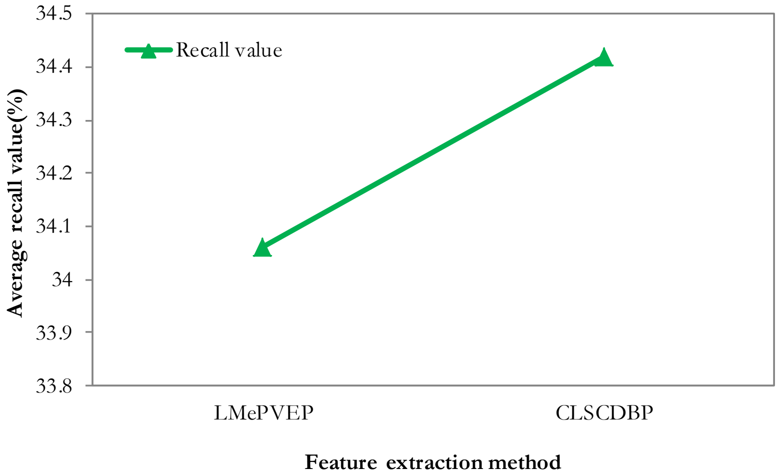

Figure 7. Recall value Comparison of combined ultrasound kidney images

The reported analysis that is shown from Figure 4 to Figure 8 confirms that the discriminative power of the proposed CLSCDBP is noteworthy. Besides the analysis with precision and recall, the single value measure is more appropriate to compare the performance of the retrieval systems. The substantiation of the performance can be easily drawn from the single value measure rather than the graph. The important single value measure is the Mean Average Precision (MAP) [40]. The MAP combines the impact of precision and recall measures into the single value. The MAP is highly depended on the rank of the relevant images. The MAP value is computed using the Equation 7. It is rated in the scale of 0 to 1. The perfect retrieval yields the value 1. The value 0 worsens the performance.

$$MAP = \frac{1}{NQ}\sum_{q=1}^{NQ} AP(q) \tag{7}$$

where AP(q) is the average precision for a query image q; NQ is the number of query images.

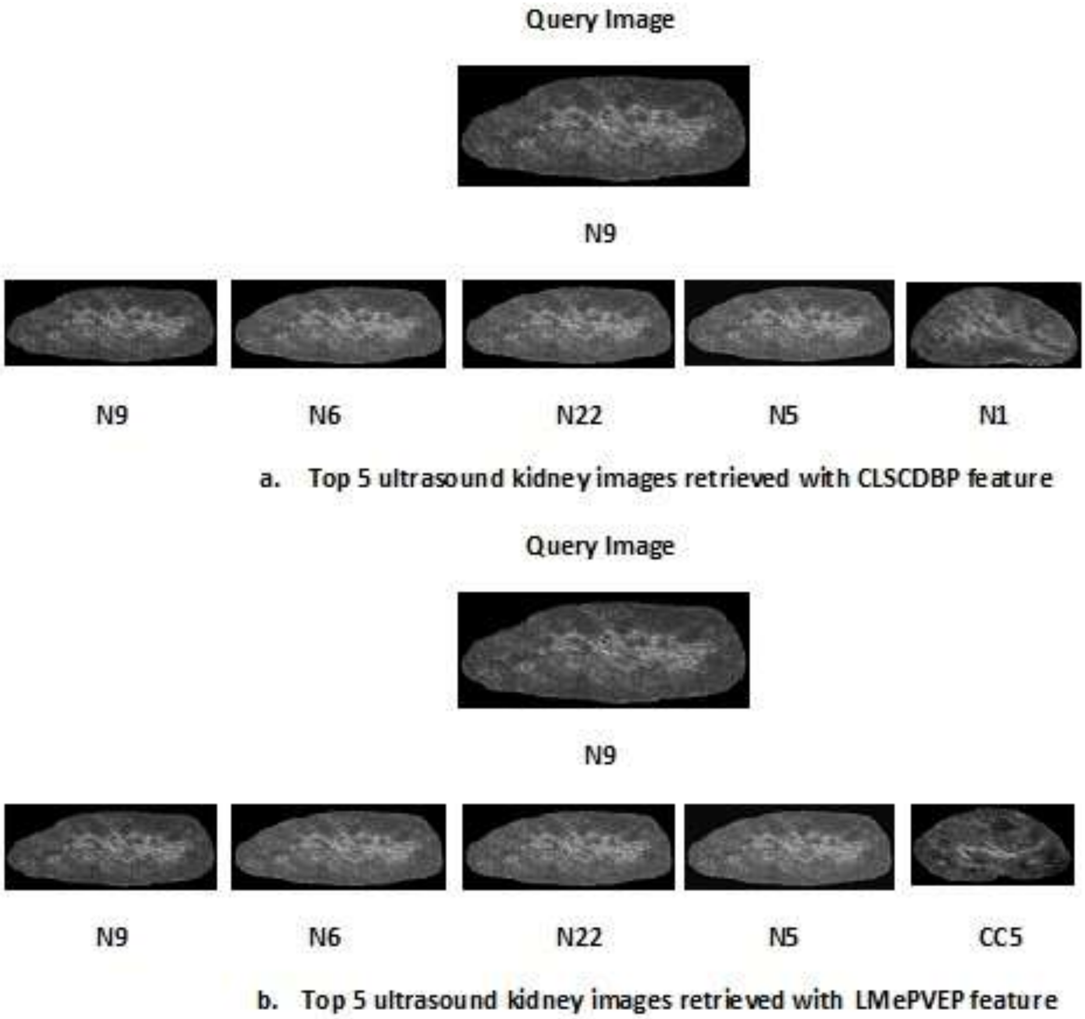

Figure 8. Top 5 Retrieval Results of ultrasound kidney image retrieval system with CLSCDBP and LMePVEP features

The term AP(q) is computed by taking the mean of the precision with every relevant images of q and it is given in the Equation 8.

$$AP(q) = \frac{1}{NR}\sum_{q=1}^{NR} P_q R_i \tag{8}$$

where R_i is the recall after the i^{th} relevant images retrieved.

The MAP value of the three categories of the ultrasound kidney images with two image retrieval methods are given in Table 1.

Table 1. The MAP comparison of CLSCDBP and LMePVEP features based ultrasound kidney images retrieval system

Feature Extraction Method	MAP		
	Normal	CC	MRD
CLSCDBP	0.5105	0.3895	0.5286
LMePVEP	0.4879	0.3585	0.4853

MAP = Mean Average Precision; CC = Cortical Cysts; MRD = Medical Renal Diseases

Though the MAP is the best single value measure, it does not consider the size of the entire database. Because of it, the MAP cannot predict the performance of the system with the scaled up version of the database. This problem can be rectified by another single value measure, Normalized Average Rank (NAR) [41] as it accounts the size of the database. The NAR is also rated between 0 and 1. The value 0 means the perfect retrieval and the value 1 degrades the performance. The NAR of the query q is defined in the Equation 9.

$$NAR(q) = \frac{1}{N \cdot NR}\left(\sum_{I=1}^{NR} R_i - \frac{NR(NR-1)}{2}\right) \qquad (9)$$

where N is the size of the database, NR is the number of relevant images and R_i is the Rank of the i^{th} relevant image of the query. The average NAR value (ANAR) of the CLSCDBP and LMePVEP system with the three categories of ultrasound kidney images are given in Table 2.

Table 2. The ANAR comparison of CLSCDBP and LMePVEP features based ultrasound kidney images retrieval system

Feature Extraction Method	ANAR		
	Normal	CC	MRD
CLSCDBP	0.2807	0.3632	0.2639
LMePVEP	0.2893	0.3786	0.2796

ANAR = Average Normalized Average Rank
CC = Cortical Cysts; MRD = Medical Renal Diseases

The overall comparison of the experimental work is provided in the Table 3. The average precision values in top 10 images, the average recall values in top 100 images, the MAP value , the ANAR value and the feature vector length is considered for overall comparison.

Table 3. The overall comparison of CLSCDBP and LMePVEP features based ultrasound kidney images retrieval system

Feature Extraction Method	Average precision of retrieval of top 10 images (%)	Average recall of retrieval of top 100 images (%)	[MAP, ANAR]	Feature Vector Length (n), Computational Overhead
CLSCDBP	74	34.41	[0.4797, 0.3003]	1536 (6*256), O(n)
LMePVEP	71	34.06	[0.4481, 0.3132]	1024 (4*256), O(2n)

MAP = Mean Average Precision ; ANAR = Average Normalized Average Rank; O =Big Oh Notation

From the Table 3, it is inferred that the CLSCDBP feature based ultrasound kidney image retrieval system outruns the performance of the LMePVEP based ultrasound kidney image retrieval system. This supremacy is due to the improvement in the calculation of local pattern by means of central derivative encoding in every surrounding pixel of the local region and the inclusion of macro information with global mean.

Conclusions

The image retrieval algorithm with the new Complete Local Spatial Central Derivative Binary Pattern (CLSCDBP) is proposed in this paper. The pattern encodes the central derivatives of the surrounding neighbors of the center pixel in the every 3×3 local region at 3 possible spatial distances. The local pattern becomes complete by including the global statistics information into it. The effectiveness of the feature is tested on ultrasound kidney image retrieval system. The comparison is made with the LMePVEP feature as it finds the relationships among the surrounding pixels. The results proved that the ultrasound kidney image retrieval system with the CLSCDBP feature has noteworthy improvement than LMePVEP feature. The feature extraction with higher retrieval efficiency is needed in search of information from past history. The information can be used for citation, diagnosis and surgery applications. This work suggested that CLSCDBP feature can be used as the feature extraction procedure in various medical domain applications and pattern recognition applications.

Conflict of Interest

The authors declare that they have no conflict of interest.

Acknowledgements

The authors wish to thank Dr. S. Arul Kishnamoorthy, English Professor (Retired), Kovilpatti, Tamilnadu, India for his linguistic support.

References

1. Eakins JP.Towards in intelligent image retrieval. Pattern Recognition 2002;35(1):3-14.
2. Feng D, Siu WC, Zhang HJ. Multimedia information retrieval and management-Technological fundamentals and applications. Berlin, Springer; 2003.
3. Muller H, Michoux N, Bandon D, Geissbuhler A. A review of content based image retrieval systems in medical applications-Clinical benefits and future directions. International Journal of Medical Informatics 2004;73(1):1-23.
4. Tuceryan M, Jain AK. Texture analysis, in: Chen CH, Pau LF, Wang PSP (Eds.). Handbook of Pattern Recognition and Computer Vision. Singapore: World Scientific Publishing; 1993.
5. Landeweerd GH, Gelsema ES. The Use of Nuclear Texture Parameters in the Auto-matic Analysis of Leukocytes. Pattern Recognition 1978;10:57-61.
6. Chen CC, Daponte JS, Fox MD. Fractal Feature Analysis and Classification in Medical Imaging. IEEE Transactions on Medical Imaging 1989;8:133-142.
7. Stavroul G, Mougiakakou, Ioannis K, Valavanis, Alexandra Nikita, Konstantina SN. Differential diagnosis of CT focal liver lesions using texture features, feature selection and ensemble driven classifiers. Artificial Intelligence in Medicine 2007;41(1):25-37.
8. Manikandan S, Rajamani V. A Mathematical Approach for Feature Selection and Image Retrieval of Ultra Sound Kidney Image Databases. European Journal of Scientific Research 2008;24(2):163-171.
9. Baopu Li, Max Q, Meng H. Texture analysis for ulcer detection in capsule endoscopy images. Image and Vision Computing 2009;27(9):1336-1342.
10. Sang Cheol Park, Xiao-Hui Wang, Bin Zheng. Assessment of Performance Improvement in Content-based Medical Image Retrieval Schemes Using Fractal Dimension. Academic Radiology 2009;16(10):1171-1178.
11. El-Sayed Ahmed El-Dahshan, Tamer Hosny, Abdel-Badeeh M Salem. Hybrid intelligent techniques for MRI brain images classification. Digital Signal Processing 2010;20(2):433-441.
12. Quellec G, Lamard M, Cazuguel G, Cochener B, Roux C. Wavelet optimization for content-based image retrieval in medical databases. Journal of Medical Image Analysis 2010;14:227-241.
13. Sohail ASM, Bhattacharya P, Mudur SP, Krishnamurthy S, Gilbert L. Content-based retrieval and classification of ultrasound medical images of ovarian cysts. Artificial Neural Networks in Pattern Recognition 2010;5998:173-184.
14. Júlia EEO, Alexei MCM, Guillermo CC, Ana Paula BL, Thomas MD, Arnaldo AAraújo. MammoSys: A content-based image retrieval system using breast density patterns. Computer Methods and Programs in Biomedicine 2010;99(3):289-297.
15. Kehong Yuan, Zhen Tian, Jiying Zou, Yanling Bai, Qingshan You. Brain CT image database building for computer-aided diagnosis using content-based image retrieval. Information Processing & Management 2011;47(2):176-185.

16. Zare MR, Mueen A, Woo Chaw Seng, Awedh MH. Combined Feature Extraction on Medical X-ray Images. Third International Conference on Computational Intelligence, Communication Systems and Networks (CICSyN) 2011; Bali: 264-268.
17. Yu-Ying Liu, Mei Chen, Hiroshi Ishikawa, Gadi Wollstein, Joel SS, James MR. Automated macular pathology diagnosis in retinal OCT images using multi-scale spatial pyramid and local binary patterns in texture and shape encoding. Medical Image Analysis 2011;15(5):748-759.
18. Rodrigo Pereira Ramos, Marcelo Zanchetta do Nascimento, Danilo Cesar Pereira. Texture extraction: An evaluation of ridgelet, wavelet and co-occurrence based methods applied to mammograms. Expert Systems with Applications 2012;39(12):11036-11047.
19. Muthu Rama Krishnan M, Vikram Venkatraghavan U, Rajendra Acharya, Mousumi Pal, Ranjan Rashmi Paul, Lim Choo Min, Ajoy Kumar Ray, Jyotirmoy Chatterjee, Chandan Chakraborty. Automated oral cancer identification using histopathological images: A hybrid feature extraction paradigm. Micron 2012;43(2–3):352-364.
20. Callins CC, Rajamani V. Performance Analysis of Grey Level co-occurrence matrix and co-occurrence of sum and difference histogram Probabilities for Ultra Sound Kidney Images Retrieval. European Journal of Scientific Research 2012;88(3):451-459.
21. Kumar SS, Moni RS, Rajeesh J. An automatic computer-aided diagnosis system for liver tumours on computed tomography images. Computers & Electrical Engineering 2013;39(5):1516-1526.
22. Shichong Zhou, Jun Shi, Jie Zhu, Yin Cai, Ruiling Wang. Shearlet-based texture feature extraction for classification of breast tumor in ultrasound image. Biomedical Signal Processing and Control 2013;8(6):688-696.
23. Callins Christiyana C, Rajamani V. Second order Statistical Texture Features from a New CSLBPGLCM for Ultrasound Kidney Images Retrieval. Applied Medical Informatics 2013;4(33):32-39.
24. Bi Bi, Li Zeng, Kuan Shen, Haina Jian. An effective edge extraction method using improved local binary pattern for blurry digital radiography images. NDT & E International 2013;53:26-30.
25. Ojala T, Pietikainen M, Maenpaa T. Multiresolution gray-scale and rotation invariant texture classification with local binary pattern. IEEE Transactions on Pattern Analysis and Machine Intelligence 2002;24(7):971-987.
26. Li Liu, Lingjun Zhao, Yunli Long, Gangyao Kuang, Paul Fieguth. Extended local binary patterns for texture classification. Image and Vision Computing 2012;30:86-99.
27. Tan X, Triggs B. Enhanced local texture feature sets for face recognition under difficult lighting conditions. IEEE Transactions on Image Processing 2010;19(6):1635-1650.
28. Nanni L, Lumini A, Brahnam S. Local binary patterns variants as texture descriptors for medical image analysis. Artificial Intelligence in Medicine 2010;49(2):117-125.
29. Zhang B,Gao Y, Zhao S, Liu J. Local derivative pattern versus local binary pattern: face recognition with higher-order local pattern descriptor. IEEE Transations on Image Processing 2010;19(2):533-544.
30. Shao-Hu Peng, Deok-Hwan Kim, Seok-Lyong Lee, Myung-Kwan Lim. Texture feature extraction based on a uniformity estimation method for local brightness and structure in chest CT images. Computers in Biology and Medicine 2010;40(11-12):931-942.
31. Murala S, Maheshwari RP, Balasubramanian R. Directional Binary Wavelet Patterns for Biomedical Image Indexing and Retrieval. Journal of Medical Systems 2012;36(5):2865-2879.
32. Ashish Oberoi, Varun Bakshi, Rohini Sharma, Manpreet Singh. A Framework for Medical Image Retrieval Using Local Tetra Patterns. International Journal of Engineering and Technology 2013;5(1):27-36.
33. Murala S, Jonathan Wu QM. Local ternary co-occurrence patterns: A new feature descriptor for MRI and CT image retrieval. Neurocomputing 2013;119:399-412.
34. Nosaka R, Fukui K. HEp-2 cell classification using rotation invariant co-occurrence among local binary patterns. Pattern Recognition 2014;47(7):2428-2436.
35. Murala S, Wu JQM. MRI and CT image indexing and retrieval using local mesh peak valley edge patterns. Signal Processing: Image Communication 2014;29(3):400-409.

36. Sun J, Fan G, Yu L, Wu X. Concave-convex local binary features for automatic target recognition in infrared imaginary. Eurosip Journal on Image and Video Processing 2014;23:1-13.
37. Khan IR, Ohba R. Closed form expressions for the finite difference approximations of first and higher derivatives based on Taylor series. Journal of Computational and Applied Mathematics 1999;107:179-193.
38. Ahonen T, Hadid A, Pietikäinen M. Face recognition with local binary patterns. In: Proc. European Conference on Computer Vision, Springer, Berlin, 2004; pp. 469-481.
39. Laine A, Fan J. Texture classification by wavelet packet signatures. IEEE Transactions on Pattern Analysis and Machine Intelligence 1993;15(11):1186-1191.
40. Stephen ER, Kanoulas E, Yilmaz E. Extending average precision to graded relevance judgments. SIGIR 2010; 603-610.
41. Muller H, Muller W, Squire D, Marchand-Maillet S, Pun T. Performance evaluation in content-based image retrieval: overview and proposals. Pattern Recognition Letters 2001;22(5):593-601.